Published in final edited form as:
Nat Med. 2011 May ; 17(5): 610–617. doi:10.1038/nm.2353.

B Lymphocytes Promote Insulin Resistance through Modulation of T Lymphocytes and Production of Pathogenic IgG Antibody

Daniel A. Winer[1,2,7], **Shawn Winer**[2,3,7], **Lei Shen**[1,7], **Persis P. Wadia**[4], **Jason Yantha**[3], **Geoffrey Paltser**[3], **Hubert Tsui**[3], **Ping Wu**[3], **Matthew G. Davidson**[1], **Michael N. Alonso**[1], **Hweixian Leong**[1], **Alec Glassford**[5], **Maria Caimol**[1], **Justin A. Kenkel**[1], **Thomas F. Tedder**[6], **Tracey McLaughlin**[5], **David B Miklos**[4], **H.-Michael Dosch**[3], and **Edgar G. Engleman**[1]

[1] Department of Pathology, Stanford University, Palo Alto, California, USA

[2] Department of Laboratory Medicine and Pathobiology, University Health Network, University of Toronto, Toronto, ON, Canada

[3] Neuroscience & Mental Health Program, Research Institute, The Hospital for Sick Children, University of Toronto Departments of Pediatrics & Immunology, Toronto, ON, Canada

[4] Department of Medicine, Stanford University, Palo Alto, California, USA

[5] Division of Endocrinology, Stanford University School of Medicine, Palo Alto, California, USA

[6] Department of Immunology, Duke University Medical Center, Durham, North Carolina, USA

Abstract

Chronic inflammation characterized by T cell and macrophage infiltration of visceral adipose tissue (VAT) is a hallmark of obesity associated insulin resistance and glucose intolerance. Here we demonstrate a fundamental pathogenic role for B cells in the development of these metabolic abnormalities. B cells accumulate in VAT in diet induced obese (DIO) mice, and DIO mice lacking B cells are protected from disease despite weight gain. B cell effects on glucose metabolism are mechanistically linked to activation of pro-inflammatory macrophages and T cells, and production of pathogenic IgG antibodies. Treatment with a B cell-depleting CD20 antibody attenuates disease, while transfer of DIO-IgG rapidly induces insulin resistance and glucose intolerance. Moreover, insulin resistance in obese humans is associated with a unique profile of IgG autoantibodies. These results establish the importance of B cells and adaptive immunity in insulin resistance and suggest new diagnostic and therapeutic modalities to manage the disease.

INTRODUCTION

Obesity and its associated metabolic abnormalities, including insulin resistance and type 2 diabetes (T2D), have reached epidemic proportions, adversely impacting health and global mortality rates[1]. Multiple factors contribute to reduced insulin sensitivity, but chronic

Correspondence: dan.winer@uhn.on.ca (D.A.W.); edengleman@stanford.edu (E.G.E.), Telephone: 650-723-7960, Fax: 650-725-0592;.
[7]These authors contributed equally to this work

AUTHOR CONTRIBUTIONS
D.W. and S.W. conceived the study, performed experimental work, and wrote the manuscript. L.S. was involved in experimental work, project planning and manuscript preparation. P.W., A.G., T.M., and D.M. contributed the human array data. J.Y., G.P., M.D., M.A., H.T., Pi.W., H.L., J.K., and M.C. performed experimental work; T.T. contributed the CD20 mAb and was involved in manuscript preparation. H.-M.D. financed and supervised parts of the project, and was involved in manuscript preparation; E.E. was involved in project planning, financing, supervision, data analysis, and manuscript preparation. E.E. and H.-M.D. are co-senior authors.

inflammation in visceral adipose tissue (VAT) resulting in local and systemic increases in pro-inflammatory cytokines/adipokines is a major driver[2,3].

Macrophage infiltration of VAT is a key event in the establishment of adipose inflammation and insulin resistance[4,5]. Classically activated, or M1, macrophages ($CD11c^+CD206^-$) are elevated in VAT of DIO mice and produce pro-inflammatory cytokines such as TNF-α, IL-1β, and IL-6[6–8]. T cells are also major participants in VAT inflammation, with pro-inflammatory $CD8^+$ T cells and IFN-γ producing $CD4^+$ T cells contributing to inflammation, glucose intolerance and insulin resistance in DIO mice[9–11]. On the other hand, VAT-resident $Foxp3^+$ Treg cells, which produce IL-10 and TGF-β, and IL-4/IL-13 secreting Th2 cells, can play protective roles[11–13]. Remarkably, the clonal diversity of VAT T cells is highly restricted, which suggests that an active adaptive immune response expanding potentially autoimmune T cells occurs in obese VAT[11–14].

In contrast to macrophages and T cells, little is known about the role of B cells in the development of insulin resistance despite evidence that such cells are recruited to adipose tissue shortly after initiation of a high fat diet[15] and their activation is increased in patients with T2D[16]. Here we demonstrate that B cells and IgG are important pathogenic effectors in the development of obesity-associated insulin resistance and glucose intolerance, but not of excess weight gain, in DIO mice. Manipulation of B cells, antibodies or their receptors may yield promising new therapies for the management of insulin resistance and its associated co-morbidities.

RESULTS

B cells and antibodies in diet induced obesity

We analyzed early immune cell infiltration into epididymal VAT of 6 week old C57BL/6 mice fed a high fat diet (HFD, 60% kcal) for several weeks and compared the immune cell composition to age matched C57BL/6 mice fed a normal chow diet (NCD) (Fig. 1a). HFD induced a significant accumulation of B cells in VAT by 4 weeks that was maintained after 6–12 weeks on HFD (Fig. 1a). This increase in B cells included total B cells, B-1a cells, and B2 cells. Total T cells were also increased by 4 weeks, and absolute numbers continued to rise while on a HFD, consistent with previous reports[11,15,17]. Despite the increase in absolute B cell numbers in DIO VAT, the relative proportions of B1 and non-B1 subsets were unchanged (Fig. 1a). However, DIO VAT had increased numbers and proportions of class switched mature B cells, such as IgG^+ cells, a pattern suggesting an active progressive immune process in DIO VAT (Fig. 1b).

To investigate the effects of HFD on systemic B cells, we analyzed spleens from age matched 12–18 week old HFD and NCD mice. No significant differences were seen in total spleen cell counts, or the percentages of naive IgD^+ B cells, marginal zone B cells, or IgM^+IgD^- follicular B cells (Fig. 1c). However, in contrast to DIO VAT, DIO spleens contained reduced percentages of IgM^+IgD^- cells (Fig. 1c). Consistently, total spleen B cells from DIO mice showed reduced spontaneous production of IgM antibody, but elevated IgG secretion (Fig. 1d), suggesting that HFD induces a systemic humoral immune response.

This was confirmed when we compared concentrations of immunoglobulin isotypes in serum and VAT of NCD and HFD mice. DIO mice had reduced concentrations of serum IgA, and an increase in IgG2c (Fig. 1e), a pro-inflammatory isotype present in C57BL/6, C57BL/10 and NOD mice[18]. VAT lysates from HFD mice had increased IgM compared to IgG, and a marked (>3 fold) enrichment in pro-inflammatory IgG2c (Fig. 1f). Interestingly, antibodies and antibody stained cells in VAT showed a preferred localization to regions of crown like structures (CLSs) (Fig. 1g)[19,20]. Many of these cells were at the interface of large

mononucleate and multinucleate giant macrophages and dying adipocytes inside the CLSs. CLSs appeared bathed in tissue fluid enriched for IgM and IgG, whereas the remaining fat tissue showed either very weak or no Ig staining. Enrichment of IgG and IgM in CLSs implicates antibodies in the clearance of dying adipocytes[19,20].

B cells are pathogenic in glucose metabolism in DIO mice

To assess the effect of B cells on the regulation of obesity and insulin resistance, mu heavy chain knockout mice (B^{null}), which fail to produce mature B cells, were investigated for their response to HFD started at 6 weeks of age [21]. After 8 weeks of HFD, there was no difference in body weight or VAT adipocyte size (Fig. 2a, b), but HFD B^{null} mice had a lower VAT:SAT (subcutaneous adipose tissue) fat pad weight than HFD WT mice (Fig. 2c).

Compared to HFD WT mice, 16 week old HFD B^{null} mice had lower fasting glucose (Fig. 2d) and improved glucose tolerance (Fig. 2e). Similarly, HFD B^{null} mice had reduced fasting insulin (Fig. 2f) and improved insulin sensitivity upon insulin challenge (Fig. 2g). B cell deficiency did not affect weight, fasting glucose/insulin or glucose/insulin tolerance in NCD mice (Fig. 2a, d–g), suggesting that metabolic influences of B cells require a HFD. To confirm that abnormal glucose metabolism in HFD mice is directly attributable to B cells, age matched 16–18 week HFD B^{null} mice were reconstituted *i.p.* with 1×10^7 total B cells from spleens of HFD WT mice. After 2–3 weeks, B cells reconstituted primarily VAT over spleen (Supplementary Fig. 1a) and produced low levels of serum antibody (Supplementary Fig. 1b). B cell transfer did not impact total weight (Fig. 2h). However, B^{null} mice reconstituted with DIO B cells had worsened glucose tolerance (Fig. 2h) and higher fasting insulin levels (Fig. 2h) compared to control B^{null} recipients. B cells from NCD mice failed to promote impairment in glucose homeostasis (Fig. 2i) despite similar reconstitution profiles as HFD B cells (Supplementary Fig. 1c), indicating that development of pathogenic B cells requires exposure to a HFD. Collectively, these results demonstrate a pathogenic role for HFD B cells in the promotion of obesity associated insulin resistance and glucose intolerance.

HFD B^{null} mice show reduced immune cell activation in VAT

Inflamed adipose tissue is a critical feature of insulin resistance. Since B cells reside in VAT and worsen metabolic parameters upon adoptive transfer, we examined the possibility that these cells promote inflammation in VAT. VAT total T cell or macrophage counts were similar in HFD WT and HFD B^{null} mice (Fig. 3a), but HFD B^{null} mice had fewer proinflammatory M1 macrophages (Fig. 3b). To examine the functional profiles of these immune cells, we measured cytokines known to affect insulin resistance (TNF-α and IFN-γ)[9,22,23]. The supernatants of total VAT stromal vascular cell (SVC) cultures from HFD B^{null} mice had lower levels of IFN-γ compared to HFD WT mice (Fig. 3c). The number of VAT associated $CD8^+$ T cells producing IFN-γ from HFD B^{null} mice was approximately 30% less compared to HFD WT $CD8^+$ T cells (Fig. 3d). HFD B^{null} $CD8^+$ T cells also expressed less CD107a, a cytotoxic activation marker (Fig. 3d). IFN-γ expression was variable in $CD4^+$ T cells of HFD WT and B^{null} mice (Supplementary Fig. 2a).

Supernatants of VAT SVC cultures from HFD B^{null} mice also contained less TNF-α compared to HFD WT mice (Fig. 3e). Macrophages, especially M1 macrophages, are a major source of TNF-α and its decrease in HFD B^{null} VAT is partly attributable to reduced numbers of macrophages producing this cytokine (Fig. 3e). In addition, fewer HFD B^{null} VAT macrophages expressed co-stimulatory CD86, consistent with an overall decrease in macrophage activation in these mice (Fig. 3f).

Analysis of serum revealed that concentrations of resistin and PAI-1, both previously associated with insulin resistance[24,25], were significantly lower in HFD B^{null} than WT mice (Supplementary Fig. 2b). This result suggests in DIO mice, B cells induce systemic as well as local (VAT) inflammation.

B cells modulate VAT associated T cells *in vivo*

B cell functions are influenced by other lymphocyte populations (especially T cells) and vice versa[26]. To begin to discern a role for T cells in facilitating B cell mediated glucose intolerance, we reconstituted 16 week old HFD $RAG1^{null}$ mice, which lack lymphocytes, with 1×10^7 total HFD splenic B cells. After 2 weeks, despite reconstitution (Supplementary Fig. 3), B cells failed to worsen fasting glucose, insulin, and glucose tolerance, contrasting with transfers into HFD B^{null} mice, suggesting that B cells require other lymphocytes to fully promote impairment of metabolic parameters (Fig. 3g).

B cells can activate $CD8^+$ and $CD4^+$ T cells by presenting antigen via MHC class I and MHC class II, respectively. To determine if B cell dependent T cell activation is important in the promotion of glucose intolerance, we reconstituted age matched 16 week old HFD B^{null} mice with 1×10^7 purified (>95%) HFD splenic B cells expressing either WT phenotype, lacking MHC class I, or lacking MHC class II. Two weeks post *i.p*. transfer, $CD19^+$ B cells had successfully reconstituted VAT but not spleen (Fig. 3h and Supplementary Fig. 1a). There were no significant differences in weight after adoptive transfer (Fig. 3i). However, in contrast to recipients of WT B cell grafts, recipients of either MHC class I^{null} or MHC class II^{null} B cells failed to develop glucose intolerance or hyperinsulinemia (Fig. 3i). Improved glucose homeostasis in both groups of MHC^{null} B cell recipients was associated with reduced total VAT SVC production of IFN-γ (Fig. 3j), attributable to either reduced number of VAT $CD8^+$ T cells producing IFN-γ (MHC-I^{null} recipients, Fig. 3j) or reduced numbers of VAT $CD4^+$ T cells producing IFN-γ (MHC-II^{null} recipients, Fig. 3j). The data show that B cell modulation of VAT T cells occurs in an MHC dependent manner, likely through B cell antigen presentation to T cells, and that both MHC class I ($CD8^+$ T cells) and class II ($CD4^+$ T cells) are needed for the B cells to maximally impact glucose tolerance in the adoptive transfer model.

IgG antibodies are mediators of glucose intolerance

In addition to functions in modulating T cell activation, B cells produce antibodies which are known regulators of immune function[27]. Since obesity is associated with increased IgG production and IgG^+ B cells in VAT, as well as increased concentrations of systemic and local IgG2c (Fig. 1b–f), we next investigated a possible role of IgG in glucose intolerance. IgG purified (>98% pure) from pooled sera of 16–24 week old HFD (HFD IgG) or NCD WT mice was injected *i.p*. into age matched DIO B^{null} mice. One week after transfer, IgG was present in serum of all recipient mice (Fig. 4a). Within this time frame, antibody transfer had no effect on body weight (Fig. 4b). However, HFD IgG induced a dramatic worsening of glucose tolerance, which was absent in NCD IgG recipients (Fig. 4c), arguing that pathogenic IgG specificities are induced during the course of a HFD but not NCD. This effect was associated with worsened fasting insulin, a hallmark of insulin resistance (Fig. 4c). Transferred antibodies also localized to VAT where they were in close association with CLSs (Supplementary Fig. 4a). The effects of antibody transfer on glucose metabolism were transient and, as expected based on normal IgG half life, by four weeks after transfer there was no difference in glucose tolerance or fasting insulin between IgG and control recipients (Fig. 4d).

To determine whether pathogenic antibodies arise early after the initiation of HFD, IgG was purified from 9–12 week old HFD mice (early HFD IgG), as well as from 20–24 week old

HFD mice (late HFD IgG), and injected *i.p.* into 20 week old HFD B^{null} nice. A much stronger effect on glucose tolerance and fasting insulin levels was seen with late HFD IgG, suggesting a possible role for affinity maturation of antibody or late unmasking of HFD antigen in the process (Fig. 4e). To investigate whether HFD IgG induced disease depends on HFD exposure in recipient mice, we transferred IgG into 6 week old lean mice. One week post transfer, there was little change in weight, glucose tolerance or fasting insulin levels (Fig. 4f), indicating that the effects of HFD IgG on glucose metabolism are dependent on the recipient's exposure to HFD.

To investigate the mechanism by which HFD IgG induces glucose intolerance, we first examined its impact on VAT and systemic inflammation. HFD IgG recipient mice had higher levels of TNF-α in VAT SVC cultures and more pronounced M1 macrophage polarization in VAT when compared to controls (Fig. 4g). In addition, these mice had elevated serum concentrations of pro-inflammatory mediators including MCP-3, IL-6, and GM-CSF (Supplementary Fig. 4b). IgG antibodies through their Fc portion can bind FcγRs on macrophages and directly induce macrophage oxidative burst, cytotoxicity and pro-inflammatory cytokine production[27]. To determine if the observed effect of IgG antibodies on glucose intolerance is mediated through their Fc component, we generated $F(ab')_2$ fragments from HFD IgG and compared their effect on glucose metabolism to that of HFD IgG. One week post *i.p.* transfer into age matched DIO B^{null} mice, HFD IgG $F(ab')_2$ failed to worsen glucose tolerance and fasting insulin, indicating that the pathogenic properties of HFD IgG are mediated through the Fc region (Fig. 4h). Consistent with these findings, macrophages isolated from VAT of HFD B^{null} mice stimulated with HFD IgG show an Fc dependent increase in TNF-α production *in vitro* (Fig. 4i). In contrast to HFD IgG, HFD IgM had no effect on metabolic parameters (Fig 4j). These data point to an unexpected, pathogenic role for HFD induced IgG antibody in promoting glucose intolerance and insulin resistance.

Insulin resistance is linked to distinct profiles of IgG

As HFD IgG can exert pathologic effects on insulin resistance in obese mice, we next examined if IgG autoantibodies are present in insulin resistant humans and, if so, whether they recognize a distinct cluster of antigenic targets. Invitrogen ProtoArray V5.0 chips containing more than 9000 spotted antigens were probed with serum from 32 age and weight matched overweight to obese, otherwise healthy, male human subjects (Supplementary Table 1). The two groups of subjects differed only in their insulin sensitivity as determined by a modified insulin suppression test and were defined as either insulin resistant (IR) or insulin sensitive (IS) based on their steady-state plasma glucose (SSPG) levels. 122 IgG targets were identified that differentially segregated with IR while 114 targets segregated with IS. Table 1 lists the 10 antigens most highly associated with either IR or IS in our obese male subjects. Antibodies to the top three targets segregating with IR were validated in these patients by Western blot (Supplementary Fig. 5). Remarkably, in both groups the antigens are mostly intracellular proteins, with variable tissue expression.

B cell depletion ameliorates metabolic disease

To determine if manipulation of B cells can be exploited therapeutically in obesity related insulin resistance, we treated HFD WT mice with a depleting antibody against mouse CD20 (MB20-11)[28]. Antibody was injected 6–7 weeks after initiation of HFD and the mice were maintained on a HFD. B cells, which were depleted >95% locally in VAT and systemically in spleen 8 days after injection (Fig. 5a), began to repopulate tissues by day 28 post injection; nonetheless, there was still >70% depletion. CD20 mAb treatment had no effect on weight (Fig. 5b) or total serum concentrations of IgG or IgM (Fig. 5c) by 28 days after injection. However, treated mice showed improvements in fasting glucose (Fig. 5d), glucose

tolerance (Fig. 5e), and fasting insulin (Fig. 5f). Improved glucose tolerance persisted >40 days and diminished with the return of B cells (Supplementary Fig. 6a). Consistent with a role for B cells in altering the local VAT cytokine milieu, VAT SVCs of treated mice showed reduced levels of key inflammatory mediators, IFN-γ (Fig. 5g) and TNF-α (Fig. 5h), the latter change due at least partly to reduced production by macrophages (Fig. 5i). Notably, IgG from CD20 mAb treated mice was unable to transfer metabolic disease (Supplementary Fig. 6b), suggesting that CD20 mAb treatment may lead to alterations in IgG function in addition to its other effects on B cells[29].

DISCUSSION

We discovered a fundamental role for B cells in the pathogenesis of obesity associated insulin resistance. Previous studies identified other immune cells as metabolic controllers with pathogenic potential in obesity. In healthy non-obese individuals, VAT-resident regulatory T cells and Th2 cells play a beneficial role by reducing VAT inflammation. During DIO, these cells are overwhelmed by proinflammatory $CD8^+$ and Th1 cells, which promote insulin resistance and glucose intolerance[11]. B lymphocytes can now be added to the list of immune cells participating in this process, where they activate $CD8^+$ and Th1 cells and release pathogenic antibodies.

Consistent with a previous report[15], we show that B cell accumulation in VAT occurs early (by 4 weeks). B cells worsen glucose tolerance, in part, by inducing MHC dependent proinflammatory cytokine production by both $CD4^+$ and $CD8^+$ T cells. Similar mechanisms occur in models of cancer, infection[30], and autoimmunity[28]. Since B and T cells are recruited early to VAT in response to HFD[10,15], the data support a role for B cells in modulating T cell function in DIO VAT. Alternatively, T cells could function by inducing IgG class switching in B cells. Indeed, we observed elevated levels of pro-inflammatory IgG2c in serum and VAT of HFD mice. It is also possible that cytokines or antibodies produced by B cells can directly interact with and affect insulin sensitivity in adipocytes.

B cells also exacerbate metabolic disease through production of IgG. Although autoantibodies have not been previously recognized as playing a critical role in T2D, an estimated 10% of T2D patients have antibodies to islet cell antigens, and these antibodies correlated with the need for insulin therapy[31]. Almost one third of patients with advanced T2D have autoantibodies that inhibit endothelial cell function[32]. Antibodies to GFAP, which predict insulin resistance in our array (Table 1), are also reported at higher rates in T2D[33].

We show that transfer of IgG from DIO mice to HFD B^{null} mice induces rapid local and systemic changes in inflammatory cytokine production, and skews VAT macrophages to a pro-inflammatory M1 phenotype. These effects required exposure to a HFD, suggesting that factors related to diet, possibly diet induced conditioning or induction of target autoantigens, are required for antibodies to exert their effects on glucose metabolism. Furthermore, we show that IgG antibodies induce insulin resistance through an Fc mediated process. Since DIO VAT is a site of increased apoptotic/necrotic load, and antibodies concentrate in regions of VAT CLSs, it is conceivable that interactions between antibodies and FcRs on macrophages occur in VAT and promote clearance of apoptotic/necrotic debris and inflammation[34,35]. Identification of the precise FcR responsible for IgG effects on glucose metabolism warrants further investigation. Antibodies also fix complement and recently, the complement protein C3a and its receptor C3aR on macrophages, were identified as important mediators of insulin resistance[36].

We further demonstrate that insulin resistance in obese humans is linked to autoantibodies directed against a specific profile of self-antigens. Antibodies to one of the top three hits,

GFAP, occur in approximately 30% of T2D patients[33]. Interestingly, we detected antibodies to GOSR1 in more than 70% of obese insulin resistant males (P =0.0000854). GOSR1 is an essential component of the Golgi SNAP receptor complex and functions in trafficking proteins among the endoplasmic reticulum (ER) and the Golgi[37]. It is unknown whether levels of this protein change in response to ER stress, which is thought to be a prominent initiator of insulin resistance[38]. Our array data also show distinct antigenic targets associated with insulin sensitivity raising the possibility that some IgG antibodies may be protective. It will be important to validate antigenic targets in larger cohorts.

Finally, we show that depletion of B cells with a CD20 mAb early in disease has therapeutic benefit in abnormal glucose metabolism. These results are consistent with a role for B cells early in disease pathogenesis, similar to observations in several autoimmune diseases[39]. Recently, CD20 mAb was used in the treatment of atherosclerotic lesions in Apoe^{null} and Ldlr^{null} mice[40]. In CD20 mAb experiments, beneficial effects are linked to reduced T cell activation. Consistently, we observed reduced levels of pro-inflammatory IFN-γ and TNF-α in VAT after CD20 mAb treatment.

Interestingly, total serum levels of IgM and IgG following CD20 mAb treatment were not drastically changed despite a prominent therapeutic benefit, consistent with other reports[41]. One possible explanation for this finding is that in our studies, CD20 mAb was administered by 6–7 weeks after HFD, just a few weeks after B cells significantly infiltrate VAT. Since antibodies become more pathogenic with longer exposure to HFD (Fig. 4e), it is possible that the antibodies present after early treatment were not fully pathogenic. This was verified by the inability of antibodies from animals treated with CD20 mAb to transfer metabolic disease. The lack of pathogenicity of IgG at this time point could be due to reduced affinity maturation and/or class switching[41].

Rituximab, an anti-human CD20 mAb, used in the treatment of rheumatoid arthritis as well as B cell malignancies, can cause both hyperglycemia and severe hypoglycemia[42]. Other B cell and antibody modulating agents are either approved for human use or in clinical trials, including IvIg, TACI fusion proteins, and antibodies or small molecule inhibitors to CD19, CD22, CD79a,b, BLyS, Syk, and APRIL. Our findings suggest new possible uses for such agents, and agents that modulate FcR function and signaling, in the management of obesity related glucose abnormalities.

Collectively, our data support a model wherein early recruitment of B cells promote VAT T cell activation and pro-inflammatory cytokine production which potentiate M1 macrophage polarization and insulin resistance. B cells can also exert their detrimental effects systemically through production of pathogenic IgG antibodies, which target distinct clusters of self proteins. Comparative mass sequencing of T- and B- cell antigen receptors in obesity related insulin resistance is underway, and promises to yield additional insights into the fundamental cause of this pervasive disease.

METHODS

Mice

We purchased C57BL/6 (B6), B^{null} B6 (2288, B6.129S2-*Igh-6*^{tm1Cgn}/J), MHC-I^{null}(2087, B6.129P2-B2m^{tm1Unc}), MHC-II^{null}(3239, B6.129S2-C2ta^{tm1Ccum}/J), and RAG1^{null} (2216, B6.129S7-*Rag1*^{tm1Mom}/J) mice from Jackson Laboratory and maintained them in a pathogen-free, temperature controlled, 12-h light and dark cycle environment. The mice received either NCD or HFD (Research Diets, 60 kcal% fat), beginning at 6 weeks of age. All mice used in comparative studies were males and age matched between groups within

individual experiments. Studies utilized protocols approved by the Institutional Animal Care and Use Committee of Stanford University and the Hospital for Sick Children.

B cell purification

We mechanically dissociated spleens on 70μm nylon cell strainers followed by negative selection with a mouse B cell enrichment kit (Stem cell Technologies) (Supplementary Methods)

Metabolic studies

We measured GTTs, ITTs, serum insulin, and fat cell diameter as previously described[11].

Isolation of VAT-associated immune cells and VAT lysates

We isolated VAT associated immune cells as described [11]. We cultured 2.5×10^5 to 3.5×10^5 VAT derived stromal vascular cells (SVC) for 12–16 hours in a 96-well round bottom plate in RPMI supplemented with 10% fetal calf serum for cytokine measurements. We prepared VAT lysates by homogenizing VAT tissue in RIPA lysis buffer (Santa Cruz Technologies) followed by incubation on ice for 20 min. We centrifuged the lysates at 15,000g for 10 min at 4 °C before protein quantification using a BSA protein quantification kit (Thermo-scientific).

Antibody ELISA and ELISpot

We measured IgA, IgE, IgM and IgG subclasses IgG1, IgG2b, IgG2c and IgG3 in serum or VAT lysate by ELISA, using kits from Bethyl Laboratories. The frequency of spontaneous IgM- and IgG-producing B cells in spleen was determined using mouse IgG or IgM ELISpot^{PLUS} Kits (Mabtech). See Supplementary Methods.

Cytokine measurement

We measured serum cytokines by Luminex bead assay and cytokines in the supernatants of SVC VAT cultures by ELISA according to the manufacturer's instructions (eBioscience). We performed intracellular cytokine staining as described with antibodies listed in the Supplementary Methods.[10] We acquired data on a LSR II flow cytometer (BD Biosciences) and analyzed it with FlowJo software.

Flow cytometery

We stained splenocytes or fat-associated cells for 30 min with commercial antibodies (Supplementary Methods). We gated B cell subsets as B1a: $CD19^+IgM^+IgD^-B220^{-/lo}$ $CD5^+$; B1b: $CD19^+IgM^+IgD^-B220^{-/lo}$ $CD5^-$; B2/non-B1: all other $CD19^+$ cells. Splenic MZ B cells were gated as: $CD19^+IgM^+IgD^-CD21^+CD23^-$ while IgM^+IgD^-FC were defined as $CD19^+IgM^+IgD^-CD23^+CD21^-$.

Purification and transfer of IgG

We purified IgG from mouse serum using a Melon Gel IgG Spin Purification Kit (Pierce Biotechnology) and generated $F(ab')_2$ fragments using a Pierce $F(ab')_2$ Preparation Kit (Thermo Scientific) according to vendor's instructions (Supplementary Methods).

Purification and transfer of IgM

We purified IgM from serum using an IgM Purification Kit from Pierce Biotechnology (Supplementary Methods).

In vitro effects of HFD IgG

We positively selected monocytes/macrophages by CD11b microbeads (Miltenyi) from total VAT cells and then plated them at 1×10^5 cells per well in 96-well ELISA plates coated with HFD IgG (50 ug/ml). We collected the supernatant after 24 hours.

B cell depletion with CD20 mAb

Mouse CD20 mAb (MB20-11, IgG2c isotype) was provided by Dr. Thomas Tedder. We suspended sterile CD20 mAb and isotype control (Southern Biotech) at 100 μg in 100 μl PBS and administered to HFD mice *i.v.* via retro-orbital injection. No significant differences were identified between isotype treated and PBS treated mice, and these data were pooled in the control population.

Histology and immunohistochemistry

We fixed and stained VAT as previously described[11]. IgG (Vector) and IgM (Sigma) stains were performed according to the manufacturer's protocol.

Western blot analysis

We ran 1 ug of recombinant purified human GOSR1, BTK (Novus) and human purified GFAP (US Biological) on SDS-PAGE and transferred it onto a PVDF membrane. We probed the blots with patient serum samples (1:10 for GOSR1 and BTK, 1:100 for GFAP) or commercial anti-GOSR1 (1:160), anti-BTK (1:500), (Abcam) and anti-GFAP (1:500, Biolegend) as positive controls. Proteins were detected using chemiluminescence (Invitrogen).

Human Subjects

We obtained sera from 32 age and BMI matched overweight to obese male subjects (Supplementary Methods). Serum samples were obtained under approval by the Stanford Internal Review Board (IRB) for Human Subjects.

Human Antibody Array

We utilized ProtoArrays Version 5.0 (Invitrogen) with 1:500 diluted human sera run according to vendor's instructions (Supplementary methods).

Statistical analyses

Statistical significance between two means utilized unpaired t tests. Statistics comparing proportions of race in human subjects utilized a Fisher exact test. Statistics for the human array are described separately. For figure legends involving multiple experiments from pooled animal tissue, the number of experiments is listed, followed by the total number of pooled mouse samples. All data are presented as mean ± s.e.m. Statistical significance was two-tailed and set at 5%.

Supplementary Material

Refer to Web version on PubMed Central for supplementary material.

Acknowledgments

We thank Donna Jones for secretarial assistance, Claudia Benike for critical review of the manuscript, Ajay Chawla for critical review of the figures, Chao Wang, Lorna Tolentino and Kartoosh Heydari for assistance with flow cytometry, and Yang Yang and Leonore Herzenberg for help in developing macrophage and B cell subset gates.

References

1. Franks PW, et al. Childhood obesity, other cardiovascular risk factors, and premature death. N Engl J Med. 2010; 362:485–493. [PubMed: 20147714]
2. Olefsky JM, Glass CK. Macrophages, inflammation, and insulin resistance. Annu Rev Physiol. 2010; 72:219–246. [PubMed: 20148674]
3. Yuan M, et al. Reversal of obesity- and diet-induced insulin resistance with salicylates or targeted disruption of Ikkbeta. Science. 2001; 293:1673–1677. [PubMed: 11533494]
4. Weisberg SP, et al. Obesity is associated with macrophage accumulation in adipose tissue. J Clin Invest. 2003; 112:1796–1808. [PubMed: 14679176]
5. Xu H, et al. Chronic inflammation in fat plays a crucial role in the development of obesity-related insulin resistance. J Clin Invest. 2003; 112:1821–1830. [PubMed: 14679177]
6. Lumeng CN, Bodzin JL, Saltiel AR. Obesity induces a phenotypic switch in adipose tissue macrophage polarization. J Clin Invest. 2007; 117:175–184. [PubMed: 17200717]
7. Lumeng CN, Deyoung SM, Bodzin JL, Saltiel AR. Increased inflammatory properties of adipose tissue macrophages recruited during diet-induced obesity. Diabetes. 2007; 56:16–23. [PubMed: 17192460]
8. Patsouris D, et al. Ablation of CD11c-positive cells normalizes insulin sensitivity in obese insulin resistant animals. Cell Metab. 2008; 8:301–309. [PubMed: 18840360]
9. Rocha VZ, et al. Interferon-gamma, a Th1 cytokine, regulates fat inflammation: a role for adaptive immunity in obesity. Circ Res. 2008; 103:467–476. [PubMed: 18658050]
10. Nishimura S, et al. CD8+ effector T cells contribute to macrophage recruitment and adipose tissue inflammation in obesity. Nat Med. 2009; 15:914–920. [PubMed: 19633658]
11. Winer S, et al. Normalization of obesity-associated insulin resistance through immunotherapy. Nat Med. 2009; 15:921–929. [PubMed: 19633657]
12. Feuerer M, et al. Lean, but not obese, fat is enriched for a unique population of regulatory T cells that affect metabolic parameters. Nat Med. 2009; 15:930–939. [PubMed: 19633656]
13. Ilan Y, et al. Induction of regulatory T cells decreases adipose inflammation and alleviates insulin resistance in ob/ob mice. Proc Natl Acad Sci U S A. 2010; 107:9765–9770. [PubMed: 20445103]
14. Yang H, et al. Obesity increases the production of proinflammatory mediators from adipose tissue T cells and compromises TCR repertoire diversity: implications for systemic inflammation and insulin resistance. J Immunol. 2010; 185:1836–1845. [PubMed: 20581149]
15. Duffaut C, Galitzky J, Lafontan M, Bouloumie A. Unexpected trafficking of immune cells within the adipose tissue during the onset of obesity. Biochem Biophys Res Commun. 2009; 384:482–485. [PubMed: 19422792]
16. Jagannathan M, et al. Toll-like receptors regulate B cell cytokine production in patients with diabetes. Diabetologia. 2010; 53:1461–1471. [PubMed: 20383694]
17. Caspar-Bauguil S, et al. Adipose tissues as an ancestral immune organ: site-specific change in obesity. FEBS Lett. 2005; 579:3487–3492. [PubMed: 15953605]
18. Martin RM, Brady JL, Lew AM. The need for IgG2c specific antiserum when isotyping antibodies from C57BL/6 and NOD mice. J Immunol Methods. 1998; 212:187–192. [PubMed: 9672206]
19. Cinti S, et al. Adipocyte death defines macrophage localization and function in adipose tissue of obese mice and humans. J Lipid Res. 2005; 46:2347–2355. [PubMed: 16150820]
20. Strissel KJ, et al. Adipocyte death, adipose tissue remodeling, and obesity complications. Diabetes. 2007; 56:2910–2918. [PubMed: 17848624]
21. Kitamura D, Roes J, Kuhn R, Rajewsky K. A B cell-deficient mouse by targeted disruption of the membrane exon of the immunoglobulin mu chain gene. Nature. 1991; 350:423–426. [PubMed: 1901381]
22. Hotamisligil GS, Shargill NS, Spiegelman BM. Adipose expression of tumor necrosis factor-alpha: direct role in obesity-linked insulin resistance. Science. 1993; 259:87–91. [PubMed: 7678183]
23. Cintra DE, et al. Interleukin-10 is a protective factor against diet-induced insulin resistance in liver. J Hepatol. 2008; 48:628–637. [PubMed: 18267346]

24. Steppan CM, et al. The hormone resistin links obesity to diabetes. Nature. 2001; 409:307–312. [PubMed: 11201732]
25. Ma LJ, et al. Prevention of obesity and insulin resistance in mice lacking plasminogen activator inhibitor 1. Diabetes. 2004; 53:336–346. [PubMed: 14747283]
26. LeBien TW, Tedder TF. B lymphocytes: how they develop and function. Blood. 2008; 112:1570–1580. [PubMed: 18725575]
27. Nimmerjahn F, Ravetch JV. Fcgamma receptors as regulators of immune responses. Nat Rev Immunol. 2008; 8:34–47. [PubMed: 18064051]
28. Bouaziz JD, et al. Therapeutic B cell depletion impairs adaptive and autoreactive CD4+ T cell activation in mice. Proc Natl Acad Sci U S A. 2007; 104:20878–20883. [PubMed: 18093919]
29. Matsushita T, Yanaba K, Bouaziz JD, Fujimoto M, Tedder TF. Regulatory B cells inhibit EAE initiation in mice while other B cells promote disease progression. J Clin Invest. 2008; 118:3420–3430. [PubMed: 18802481]
30. DiLillo DJ, Yanaba K, Tedder TF. B cells are required for optimal CD4+ and CD8+ T cell tumor immunity: therapeutic B cell depletion enhances B16 melanoma growth in mice. J Immunol. 2010; 184:4006–4016. [PubMed: 20194720]
31. Falorni A, et al. Autoantibody recognition of COOH-terminal epitopes of GAD65 marks the risk for insulin requirement in adult-onset diabetes mellitus. J Clin Endocrinol Metab. 2000; 85:309–316. [PubMed: 10634404]
32. Zimering MB, Pan Z. Autoantibodies in type 2 diabetes induce stress fiber formation and apoptosis in endothelial cells. J Clin Endocrinol Metab. 2009; 94:2171–2177. [PubMed: 19293267]
33. Gomez-Tourino I, et al. Autoantibodies to glial fibrillary acid protein and S100beta in diabetic patients. Diabet Med. 2010; 27:246–248. [PubMed: 20546276]
34. Alkhouri N, et al. Adipocyte apoptosis, a link between obesity, insulin resistance, and hepatic steatosis. J Biol Chem. 2010; 285:3428–3438. [PubMed: 19940134]
35. Wueest S, et al. Deletion of Fas in adipocytes relieves adipose tissue inflammation and hepatic manifestations of obesity in mice. J Clin Invest. 2010; 120:191–202. [PubMed: 19955656]
36. Mamane Y, et al. The C3a anaphylatoxin receptor is a key mediator of insulin resistance and functions by modulating adipose tissue macrophage infiltration and activation. Diabetes. 2009; 58:2006–2017. [PubMed: 19581423]
37. Hay JC, Chao DS, Kuo CS, Scheller RH. Protein interactions regulating vesicle transport between the endoplasmic reticulum and Golgi apparatus in mammalian cells. Cell. 1997; 89:149–158. [PubMed: 9094723]
38. Hotamisligil GS. Endoplasmic reticulum stress and the inflammatory basis of metabolic disease. Cell. 2010; 140:900–917. [PubMed: 20303879]
39. Yanaba K, et al. B-lymphocyte contributions to human autoimmune disease. Immunol Rev. 2008; 223:284–299. [PubMed: 18613843]
40. Ait-Oufella H, et al. B cell depletion reduces the development of atherosclerosis in mice. J Exp Med. 2010; 207:1579–1587. [PubMed: 20603314]
41. DiLillo DJ, et al. Maintenance of long-lived plasma cells and serological memory despite mature and memory B cell depletion during CD20 immunotherapy in mice. J Immunol. 2008; 180:361–371. [PubMed: 18097037]
42. Hussain BM, Geetha N, Lali V, Pandey M. Rituximab induced hypoglycemia in non-Hodgkin's lymphoma. World J Surg Oncol. 2006; 4:89. [PubMed: 17156470]

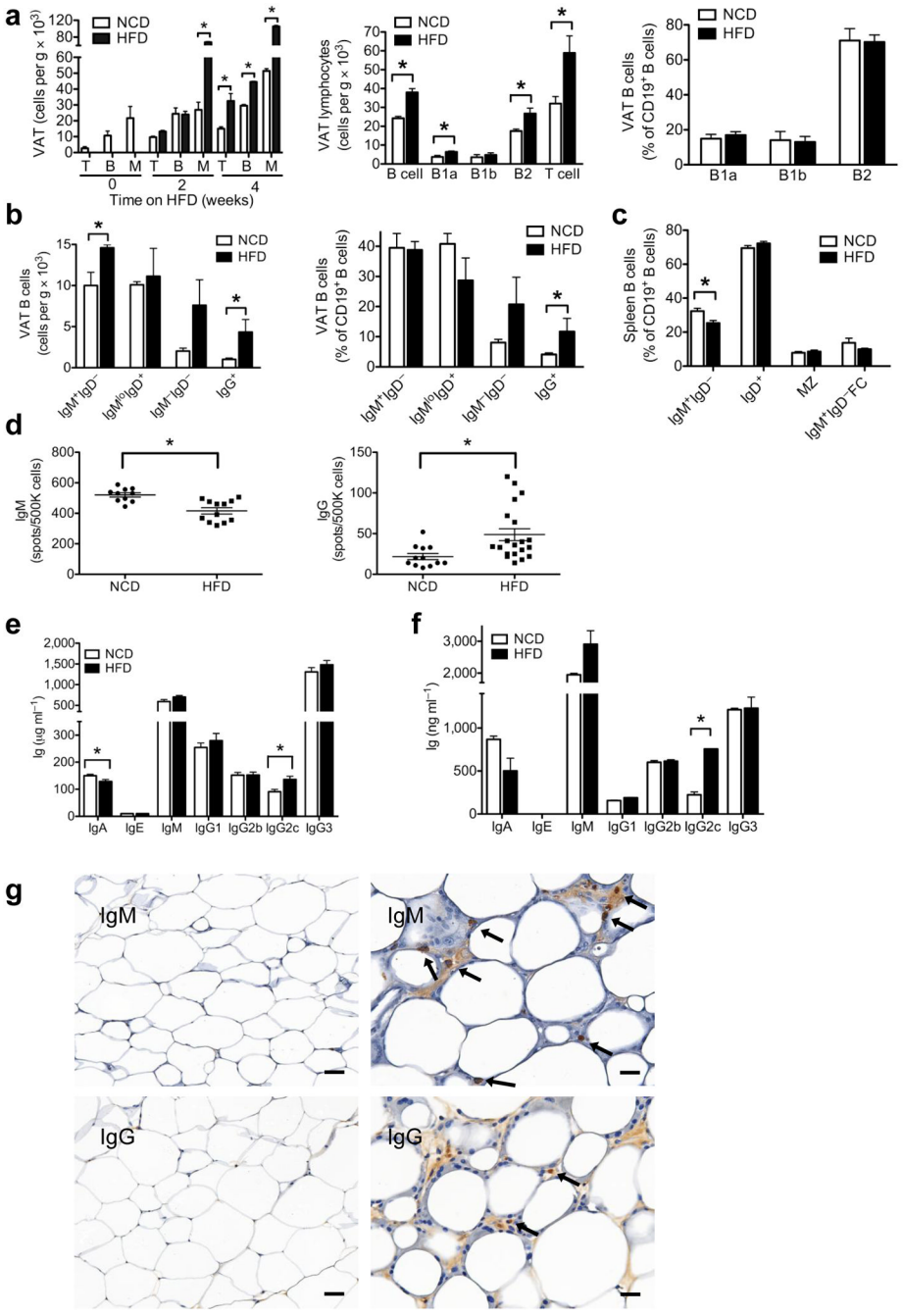

Figure 1. B cell and antibody profile in DIO mice

(**a**) Time course of T cell (T), B cell (B) and monocyte (M) infiltration of VAT after initiation of HFD (left, 2 experiments, 5 mice, *$P < 0.05$). B cell subsets in VAT in response to 6–12 weeks of HFD in absolute numbers (middle) of B cells (*$P = 0.005$), B1a cells (*$P = 0.04$), B1b cells, non-B1 cells/B2 (*$P = 0.04$) and T cells (*$P = 0.03$), and in percentages of $CD19^+$ cells (right); middle and right, 3 experiments, 9 mice. (**b**) VAT B cells in absolute numbers (left,*$P < 0.05$) and proportion of $CD19^+$ cells (right, *$P < 0.05$); left and right, 3 experiments each, 9 mice. (**c**) Spleen B cell subsets in response to HFD (MZ, marginal zone; FC, follicular cells, *$P = 0.01$, $n = 5$). (**d**) Spontaneous production of IgM (left, *$P = 0.0006$) and IgG (*$P = 0.01$) from mouse splenocytes (**e**) Serum antibody concentrations in mice:

IgA (*P = 0.03) and IgG2c (*P = 0.004) (n = 10). (**f**) Antibody subtypes in VAT lysates from mice (*P = 0.0001) (2 experiments, 5 mice). (**g**) IgM (top left) and IgG (bottom left) staining in VAT of HFD mice in regions of few and multiple CLSs (IgM top right; IgG bottom right) (arrows indicate antibody stained cells, bar 50 μm left and 25 μm right). Graphs are means ± s.e.m.

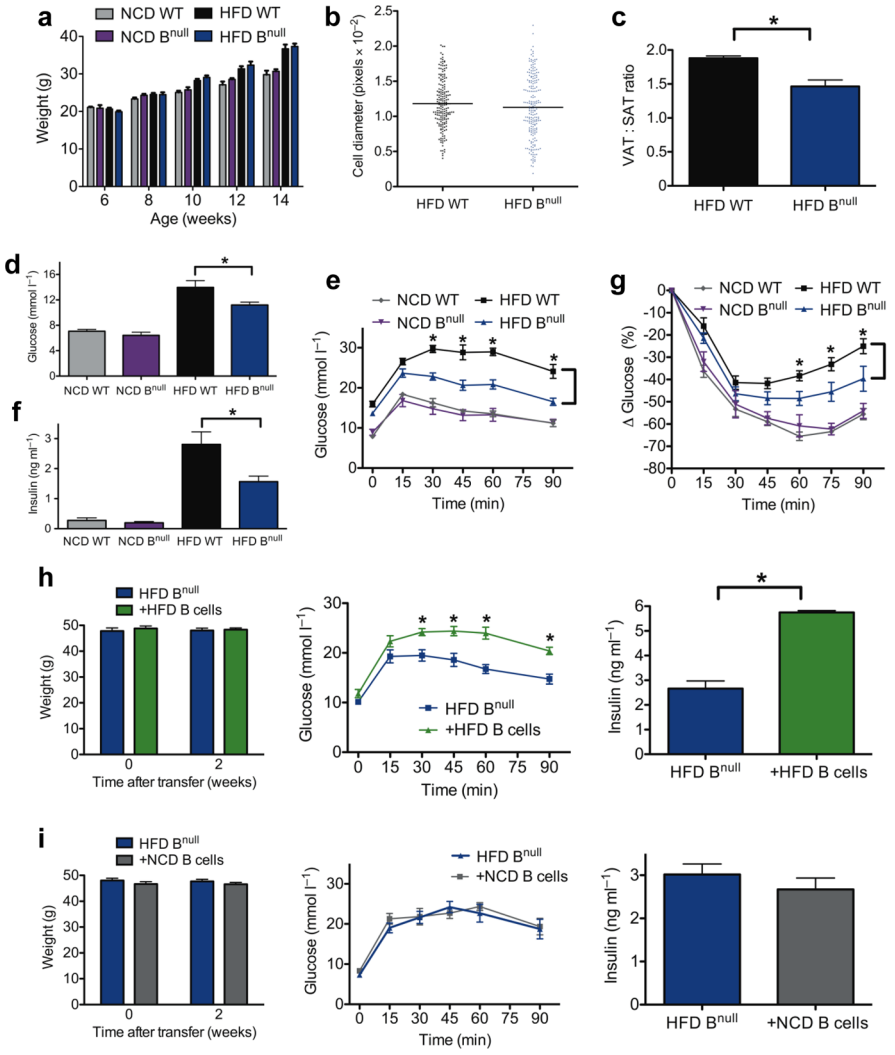

Figure 2. B cell deficiency modulates glucose metabolism in DIO mice

(**a**) Body weights of WT and B^{null} mice over time (n = 10 per group). (**b**) Relative fat cell diameter of 14–18 week old HFD mice (n = 3). (**c**) Ratio of epididymal VAT and SAT pad weights in HFD mice (*P = 0.004, n = 10) (**d**) Fasting glucose (*P = 0.04, n = 10) and (**e**) glucose tolerance test (GTT) of WT or B^{null} mice on NCD or HFD (*P < 0.05, representative GTT from 3 experiments, n=10 per group on HFD and 2 experiments, n=5 per group on NCD). (**f**) Fasting serum insulin concentrations of 16 week old WT or B^{null} mice on NCD or HFD (*P = 0.04, n = 10). (**g**) Insulin tolerance test (ITT) in WT or B^{null} mice on NCD or HFD (*P < 0.05, n = 5 per group). (**h**) Body weight (left), GTT (middle, *P < 0.05, n = 6), and fasting insulin (right, *P = 0.02, n = 6) of HFD B^{null} mice 2 weeks following reconstitution with HFD WT B cells (representative of 3 independent experiments). (**i**) Body weight (left), GTT (middle, n = 5), and fasting insulin (right, n = 5) of HFD B^{null} mice 2 weeks following reconstitution with NCD WT B cells (representative of 2 independent experiments). Graphs are means ± s.e.m.

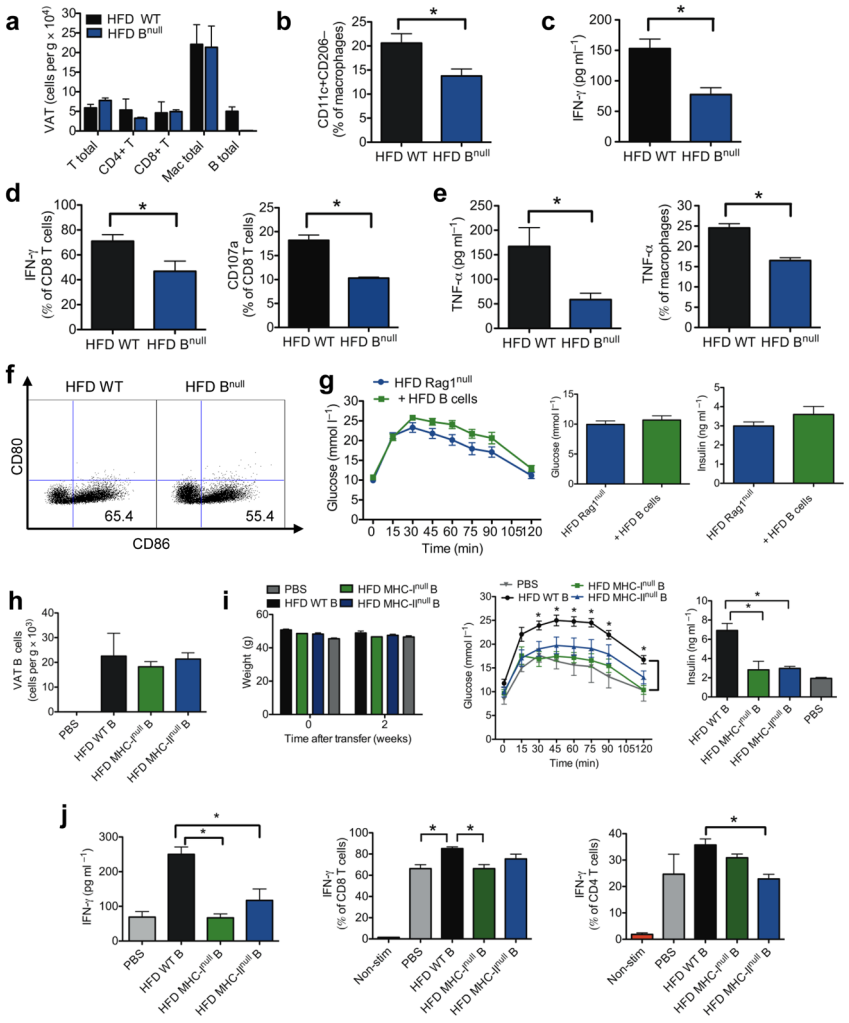

Figure 3. B cells influence VAT T cell and macrophage function

(**a**) Numbers of cell subsets in VAT of 14–18 week old mice (4 experiments, 10 mice). (**b**) Percentage of VAT macrophages ($CD11b^+F4/80^+Gr\text{-}1^-$) with M1 phenotype (*$P$ = 0.049, 3 experiments, 8 mice). (**c**) IFN-γ production from SVC cultures of VAT (3 experiments, 9 mice, *P = 0.02). (**d**) Intracellular IFN-γ staining of $CD8^+$ T cells isolated from VAT (left, 4 experiments,10 mice, *P = 0.04) and percentage of total VAT $CD8^+$ T cells expressing CD107a (right, *P = 0.02, 2 experiments, 6 mice). (**e**) TNF-α production from VAT SVC cultures (left, *P = 0.04, 2 experiments, 6 mice) and intracellular staining of TNF-α in VAT macrophages (right, 2 experiments, 6 mice, *P = 0.02). (**f**) CD80 and CD86 expression on VAT macrophages (representative of 3 experiments, 9 mice). (**g**) GTT (left), fasting glucose (middle) and fasting insulin (right) of recipient HFD RAG^{null} mice 2 weeks after transfer of HFD B cells (n = 10). (**h**) $CD19^+$ B cells in VAT of B^{null} mice 2 weeks after reconstitution with various B cells (3 experiments, 9 mice). (**i**) Weights (left), GTT (middle) and fasting insulin (right) of recipient mice 2 weeks after transfer of various B cells (*P < 0.05, representative of 3 experiments, n = 3 per group). (**j**) IFN-γ production from VAT SVC cultures (left), and intracellular IFN-γ in VAT $CD8^+$ T cells (middle) and VAT $CD4^+$ T cells (right) isolated from recipient B^{null} mice receiving either PBS orvarious B cells (*P < 0.05, 2 experiments, 6 mice). Graphs are means ± s.e.m.

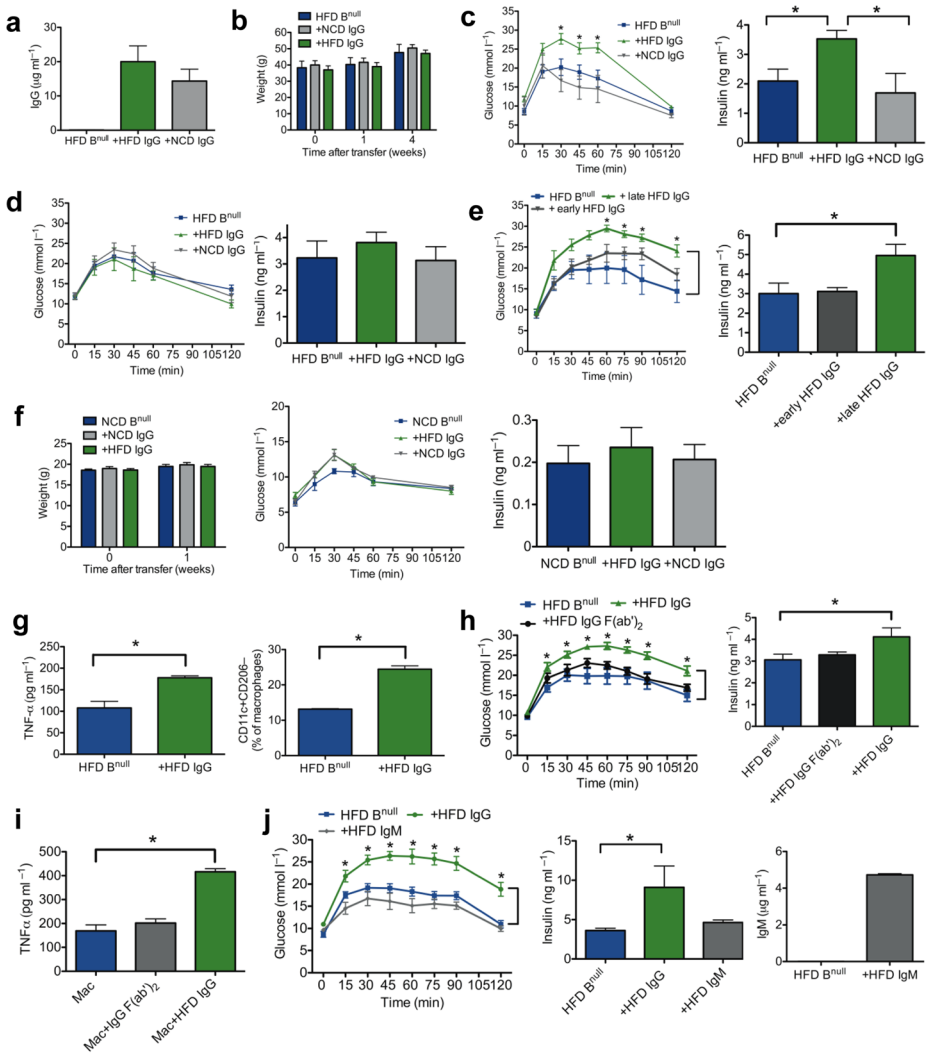

Figure 4. IgG antibodies from obese mice induce abnormal glucose metabolism in recipient B^{null} mice

(**a**) Serum concentration of IgG in B^{null} mice one week following *i.p.* IgG injection (n = 3). (**b**) Body weights of HFD B^{null} recipient mice after IgG transfer (representative of 3 experiments, n = 4). (**c**) GTT (left, * $P < 0.05$) and fasting insulin (right, *$P < 0.05$) one week following transfer of IgG into 16 week old HFD B^{null} mice (representative of 3 experiments, n = 4). (**d**) GTT (left) and fasting insulin (right) four weeks following transfer of IgG (representative of 2 experiments, n = 4). (**e**) GTT (left, *$P < 0.05$) and fasting insulin (right, *$P = 0.048$) one week following transfer of late or early IgG (n = 5). (**f**) Weights (left), GTT (center), and fasting insulin (right) of 6 week old NCD B^{null} mice 1 week after IgG transfer (representative of 2 experiments, n = 4). (**g**) TNF-α from VAT SVC cultures (left, *$P = 0.04$, 2 experiments, 6 mice) and M1 macrophages in HFD B^{null} VAT one week after IgG transfer (right, *$P = 0.007$, 2 experiments, 6 mice). (**h**) GTT (left, *$P < 0.05$) and fasting insulin (right, *$P = 0.04$) one week after transfer of HFD Ig (n =5). (**i**) TNF-α from HFD B^{null} VAT macrophages stimulated *in vitro* with HFD IgG (*P= 0.007), or HFD F(ab ′)$_2$ (n = 3). **j**) GTT (left) and fasting insulin (middle) of HFD B^{null} mice 1 week after receiving HFD Ig (n = 5, *$P < 0.05$). Serum concentration (right) of IgM in HFD B^{null} mice 1 week following IgM injection (n = 3). Graphs are means ± s.e.m.

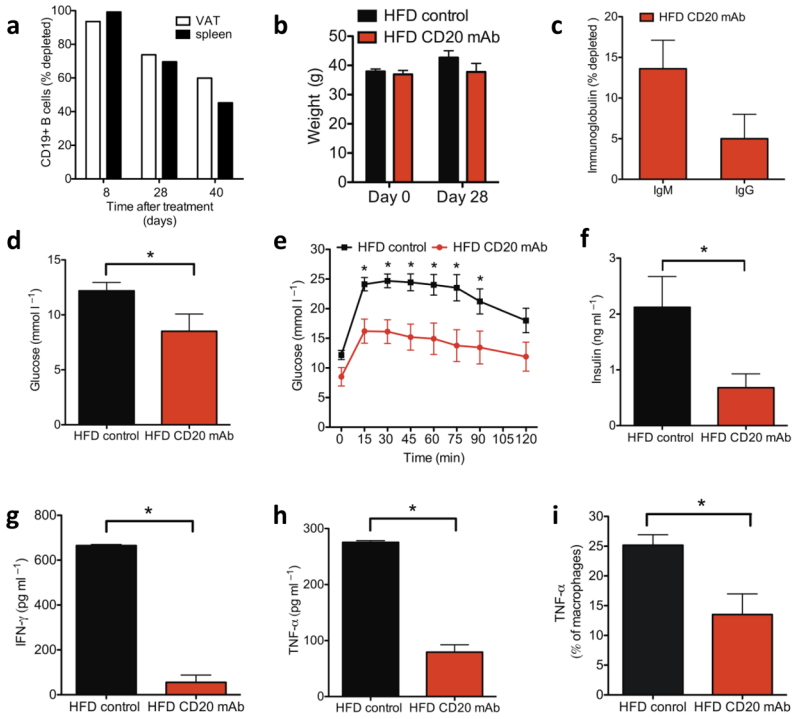

Figure 5. A CD20-specific B cell-depleting antibody improves obesity induced glucose abnormalities

Age matched 12–13 week old (6–7 weeks on HFD) HFD WT mice were treated with MB20-11 CD20 mAb (100 μg i.v.). (**a**) Percentage of $CD19^+$ cells depleted in VAT and spleen ≥8 days following administration of CD20 mAb. (**b**) Weights of mice and (**c**) percentage depletion of IgG and IgM antibody in serum 28 days post CD20 mAb treatment (representative of two experiments, $n = 5$). (**d**) Fasting glucose (*$P = 0.06$), (**e**) GTT (*$P < 0.05$) and (**f**) fasting insulin (*$P = 0.04$) in HFD WT mice 28 days after receiving either CD20 mAb or control (IgG2c or PBS) (representative of two experiments, $n = 5$). (**g**, **h**) IFN-γ (*$P = 0.003$) and TNF-α (*$P = 0.005$) production from SVC cultures of VAT isolated from 17 week old mice treated with CD20 mAb at 13 weeks of age (2 experiments, 8 mice). **i**) Percentage of VAT macrophages expressing TNF-α 4 weeks after treatment with CD20 mAb (*$P = 0.01$, 2 experiments, 8 mice). Graphs are means ± s.e.m.

Table 1

Top ten antibody targets most strongly associated with insulin resistance (IR, top) and with insulin sensitivity (IS, bottom) in human male subjects

ANTIGEN	P-Value	IR Prevalence	IS Prevalence
GOSR1	8.54E-05	72.22%	11.11%
BTK	0.001224	50%	5.56%
GFAP	0.001224	50%	5.56%
ASPA	0.003399	44.44%	5.56%
NIF3L1	0.003399	44.44%	5.56%
PGD	0.003399	44.44%	5.56%
ALDH16A1	0.003399	44.44%	5.56%
KCNAB1	0.003399	44.44%	5.56%
RNA_POLYMERASE	0.004574	61.11%	16.67%
GSTA3	0.004574	61.11%	16.67%
ANTIGEN	**P-Value**	**IR Prevalence**	**IS Prevalence**
CTNNA1	0.001027	11.11%	61.11%
CDC37	0.001224	5.56%	50%
LGALS14	0.001224	5.56%	50%
BM88	0.002961	11.11%	55.56%
NCBP2	0.002961	11.11%	55.56%
PDDC1	0.003399	5.56%	44.44%
ALS2CR8	0.003399	5.56%	44.44%
PAFAH G SUBUNIT	0.004574	16.67%	61.11%
XRCC4	0.006057	27.78%	72.22%
Influenza A Antigen (H3N2)	0.007749	44.44%	88.89%